DEVELOPMENT OF A HIGH PRECISION CO-PLANAR XY STAGE WITH MULTI-DEGREE-OF-FREEDOM SENSING SYSTEM

Kuang-Chao Fan, Hung-Yu Wang, Shih-Hsin Hsu and Li-Min Chen*

Department of Mechanical Engineering, National Taiwan University, Taipei 10617, Taiwan
** Corresponding author: fan@ntu.edu.tw*

Abstract:
With the continuing trend toward device miniaturization in many engineering and scientific fields, the need to accomplish highly-precise measurements at the micro- or nano scale has emerged as a critical concern. In practice, the accuracy of high-precision machines is affected by the Abbe principle due to inevitable angular errors during motion. Therefore, this study focuses on the development of a high precision nanometer level co-planar XY stage with miniature multi-degree-of-freedom measurement system (MDFMS).

The symmetric structural design of the co-planar stage is considered to eliminate the structure deformation due to force and temperature changes. The MDFMS is constructed by a wavelength corrected Michelson interferometer and a coaxial dual-axis autocollimator. The wavelength correction of the miniature laser interferometer is achieved by employing a holographic grating so that the real-time mean wavelength of the laser diode can be detected to the resolution of 0.001 nm. Controlling the temperature within 20 ± 2℃, the wavelength stability is less than 10^{-6}. Conventional complicated frequency stabilization technique is no more needed. In addition, using the laser diode as the light source, the MDFMS can be reduced to a small physical size so as to be used as the feedback sensor in the stage. The autocollimator has a resolution of 0.1 arc-sec and accuracy of ±0.3 arc-sec within the range of ±30 arc-sec in both axes. These detected angular errors can be used to compensate for the Abbe error if the functional point of the stage is at a certain Z-height, or called the Abbe offset. Experimental results show that, after error compensations, the positioning error can be controlled to ±20 nm for the travel up to 20 mm long.

Keywords: Co-planar Stage, Abbé Error, Multi-degree-of-freedom Measurement System (MDFMS), Wavelength Correction

1. INTRODUCTION

Micro/nano-positioning systems with nanometer level resolution and accuracy are critically important for nanotechnology. Many nano-positioning stages are wildly used in various applications, such as scanning probe microscope [1, 2], nanotechnologies [3, 4], semiconductor, optical alignment [5], and coordinate measuring machines, etc. [6, 7]. In each of these machines, the XY stage is an important motion module.

In general, an XY stage can be divided into two main classes, namely the stack-up type and the co-planar type. The stack-up type usually couples two linear stages with one stacked on top of the other and provides displacements in the X- and Y-directions, respectively [8-11]. Even though the two stages may individually possess a nanometer scale positioning accuracy, however, it is extremely difficult to achieve good positioning performance due to assembly errors, component misalignment, control error, and so on. In practice, the performance of high-precision measurement and fabrication machines is constrained by the Abbe principle.

Abbe error is one of the most important sources of uncertainty in dimensional metrology applications aimed at the nanometer scale [12]. Traditionally, the effects of errors on the measurement performance of high-precision co-planar XY stage is usually mitigated using a feed-forward compensation technique, in which the positioning errors obtained through a prior calibration process are stored and then used to compensate for the error budget [13]. However, such an approach can only compensate for the mean systematic errors of the system. In order to compensate for the Abbe errors, which are transient and caused by angular deviations, the Abbe offset must be determined in advance. However, in many cases, the Abbe offset can only be guessed for reasons related to the definition of the measurement line of the displacement sensor or the measurement trace of the structure localization sensor [14]. Furthermore, the angular deviations which lead to the Abbe errors are not constant but vary in accordance with changes in the ambient temperature.

In nanometer scale measurement systems, heterodyne laser interferometers provide the means to detect the displacement of the stage with a high metric resolution and precision even over long measurement distances [15]. However, such interferometers have a large size and a high cost, and are therefore constrained to be used only in such high-end applications as IC steppers, and so on. Compared to heterodyne laser systems, homodyne laser interferometers have many advantages, including an improved ease of use, a simpler structure and a lower cost [16, 17]. However, the stability, resolution and accuracy of homodyne laser interferometers are all susceptible to the environment, vibration, the structural design of the equipment, and other factors [18].

In this report, the high precision XY co-planar stage is presented. In order to achieve a long-stroke and nano-positioning travel, each axis is driven by an ultrasonic motor with specific commands for required motions. A MDFMS has been developed not only for measuring the displacement to nanometer resolution but also for detecting the pitch and yaw errors of each axis for Abbe error compensation.

2. STRUCTURE DESIGN OF THE CO-PLANAR XY STAGE

The X-Y stage is a co-planar type mechanism comprising two linear stages, four linear slides, two

ultrasonic motors, two MDFMS, and mechanical parts, as shown in Figure 1.

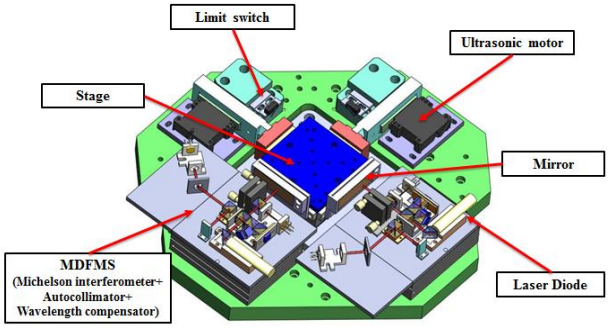

Fig. 1: Basic configuration of XY co-planar stage

2.1 Co-planar XY stage

Figure 1 illustrates the structure of the co-planar XY stage. As shown, two sides of the table are connected to the x- and y-axis extension arms supported by linear stages, which are driven by ultrasonic motors (Nanomotion Co., Model HR4) and guided by linear slides (THK Co. model SRS9N). The other two sides of the table are mounted with respective long reflection mirrors, which motions are detected by the corresponding MDFMS proposed in the present study for obtaining the position, pitch and yaw motions. The moving table slides over a common base plane, which is precisely ground to a flatness of less than 1 μm and isolated from the drive and sensing blocks. In order to ensure a smooth motion of the table, concave grooves are formed on the base plane using a scraping process and are filled with liquid lubricant in order to minimize the sliding friction force.

2.2 The Abbe principle in XY Co-planar Stage

The famous Abbe principle is only valid for a 1D motion, but in case of a co-planar stage there are 2D motions. This study thus proposes an extended Abbe principle for a 2D motion machine:

(1) Both two measuring axes should intersect at the functional point of the machine.

(2) Each measuring axis should be in line with its corresponding motion axis.

To achieve Abbe free X-Y stage, the assembly needs to follow two procedures. Firstly, define the functional point of the stage and make sure both of measuring axes will be intersected at this point, as shown in Figure 2. Secondly, a quadrant photodetector (QPD) is employed to assist the optical alignment so that the laser beam can be adjusted to allow projecting onto the detector at the same position both at near end and far end of travel, as shown in Figure 3.

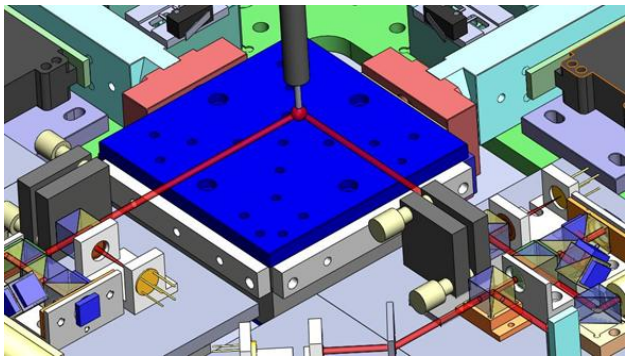

Fig. 2: Functional point of co-planar stage

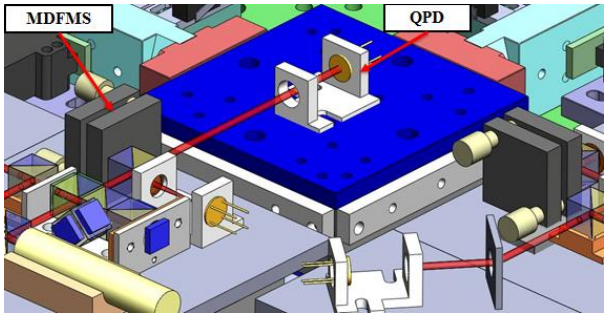

Fig. 3: Schematic diagram of laser beam alignment method

2.3 Configuration of MDFMS

Figure 4 illustrates the basic configuration of the MDFMS proposed in the present study. The system comprises a Michelson interferometer, a dual-axis autocollimator and a wavelength compensator module.

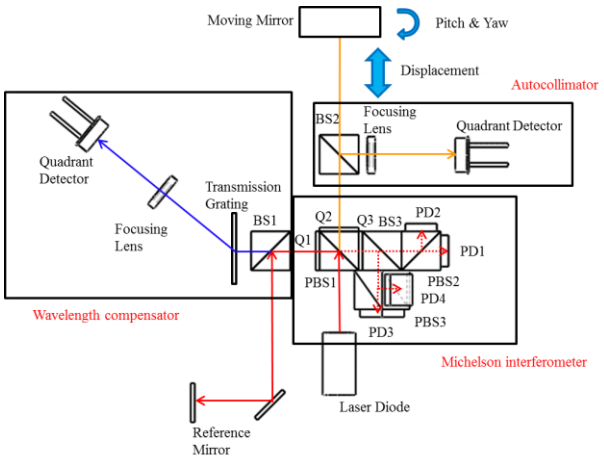

Fig. 4: Configuration of MDFMS

In the Michelson interferometer, quarter waveplates Q1 and Q2 can prevent the reflected beams returning to the laser diode due to the change of polarization of the transmited and the reflected laser beams at PBS1. Thus, the two beams reflected from the reference mirror and the moving mirror are combined at PBS1 and converted into left- and right-circularly polarized beams, respectively, by quarter waveplate Q3. A phase shift module comprising BS3, PBS2 and PBS3 then produces an interference fringe with a 90° phase shift which is detected simultaneously by photodetectors PD1 to PD4. In accordance with Jones

calculus theory, the intensity of the light incident on each PD can be expressed as:

$$I_{PD1} = A\left[1-\cos(\frac{2\pi d}{\lambda})\right] \quad (1)$$

$$I_{PD2} = A\left[1+\cos(\frac{2\pi d}{\lambda})\right] \quad (2)$$

$$I_{PD3} = A\left[1+\sin(\frac{2\pi d}{\lambda})\right] \quad (3)$$

$$I_{PD4} = A\left[1-\sin(\frac{2\pi d}{\lambda})\right] \quad (4)$$

Where, A and λ are the intensity and the wavelength of the laser beam, and d is the optical path difference of the two reflected beams.

In front of the polarizing Michelson interferometer there is an autocollimator. According to the principle of optical autocollimator as shown in Figure 5(a) and Figure 5(b), the tilted angle (θ) of the plane mirror will result in the focused spot being shifted laterally by 2fθ, where f is the focal length of the focusing lens. The built-in four-quadrant photodiode (QPD) is used as the beam spot position detector to detect the amount of spot shift. The two tilted angles of the plane mirror can then be calculated.

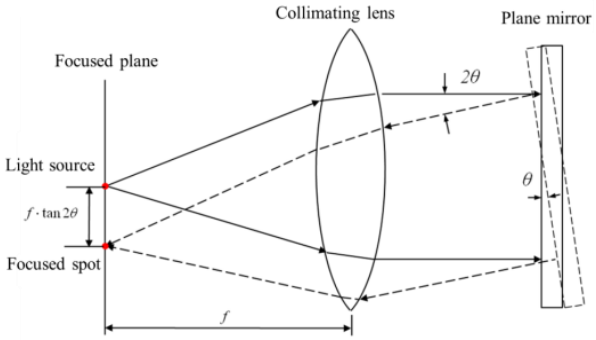

Fig. 5(a): The spot movement when the plane mirror is rotated

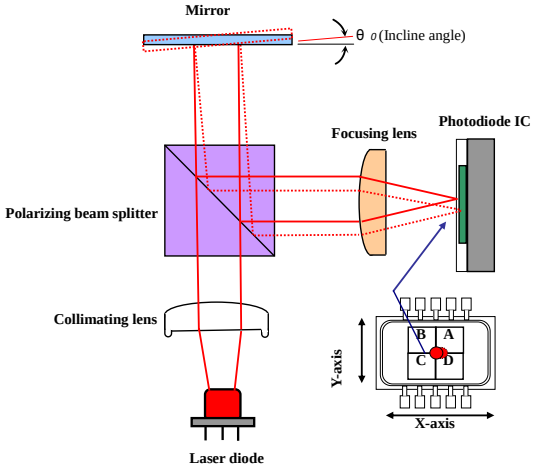

Fig. 5(b): The configuration of the autocollimator

Through the current-to-voltage converter with proper resistance, the photocurrent transformed from the photodiode will be converted to voltage for further operation. According to the location of the reflected beam projected onto the QPD, the corresponding voltages to the yaw angle (θ_y) and the pitch angle (θ_x) can be expressed by the following equations, as shown in Figure 6.

$$\theta_x = K_2[(V_A+V_B)-(V_C+V_D)] \quad (5)$$

$$\theta_y = K_2[(V_B+V_C)-(V_A+V_D)] \quad (6)$$

Therefore, the angular errors (pitch and yaw) can be measured by the autocollimator.

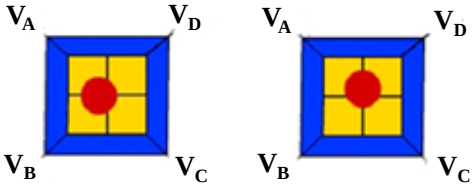

Fig. 6: The relationship between the location of beam spot and voltages (left: yaw, right: pitch)

In practice, the wavelength of the laser beam in the Michelson interferometer is not exactly equal to the nominal wavelength (i.e., 635 nm), but varies in accordance with the stability of the laser source, change in the ambient temperature, air turbulence effects, and so on. Thus, in the proposed MDFMS, the change in the laser wavelength is detected by a wavelength compensator module consisting of a transmission grating and an autocollimator (see Fig. 7(a)). Figure 7(b) illustrates the basic principle of the diffraction grating. As shown, a variation in the wavelength results in a difference in the diffraction angle, which can be measured by the autocollimator. Having measured the diffraction angle, the wavelength is determined from the diffraction equation as

$$d\left(\sin\theta_i+\sin\theta_q\right)=m\lambda,\ \ m=0,\pm1,\pm2..... \quad (7)$$

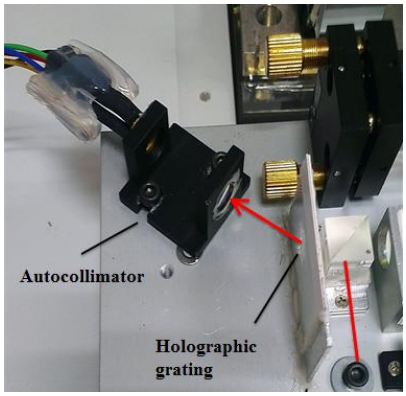

Fig. 7(a): Wavelength compensation module

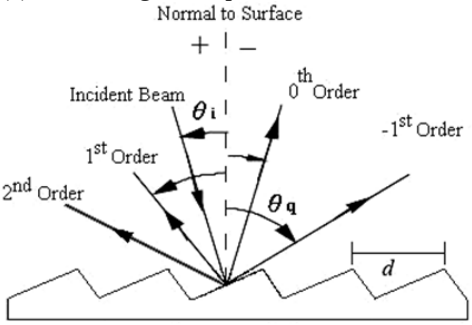

Fig. 7(b): Principle of diffraction grating

3. CALIBRATION OF MDFMS

To meet the requirement for a nanometer level positioning performance, Michelson interferometer, a wavelength compensator module and a dual-axis autocollimator were calibrated.

3.1 Michelson interferometer calibration

The Michelson interferometer was calibrated using the following two-step procedure. Firstly, the direction of the laser beam was adjusted with the assistance of a QPD so as to minimize the cosine error of the beam relative to the moving axis. Figure 8 shows the shift of the focus spot on the QPD surface in the vertical and horizontal directions after the beam direction adjustment along the stage travel of 20 mm. The cosine error between the laser beam and the movement axis is reduced to only 0.052 nm. Secondly, the wavelength of Michelson interferometer was calibrated with reference to a commercial laser interferometer (MI 5000 made by SIOS Co). Figure 9 shows the measured displacement by the Michelson interferometer and the SIOS interferometer measure over 10 mm of the table displacement simultaneously. By iterative approximation, the regression analysis reveals that the gradient is equal to one. Thus, the effectiveness of the wavelength compensation module is confirmed. Moreover, the normalized wavelength stability of the Michelson interferometer is found to be less than 10^{-6}.

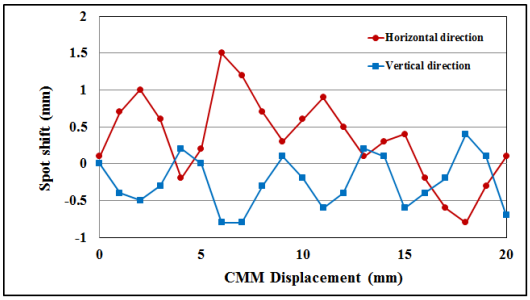

Fig. 8: Coaxial adjustment between QPD and CMM stage

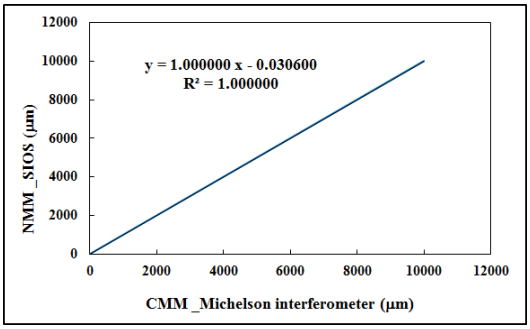

Fig. 9: Comparison of Michelson output compared with SIOS output.

3.2 Wavelength compensator module calibration

To real-time compensate the wavelength for Michelson interferometer, the QPD is employed to measure the diffraction angle variation under different wavelengths. Equation (7) shows the relationship between wavelength and diffraction angle. In order to develop the relationship, the different wavelength was adjusted by different working voltage. As shown in Figure 10, the linear equation will be used to compensate the wavelength variation which is caused by stability of the laser source, temperature variation and air turbulence.

To confirm the effectiveness of the wavelength compensation module, the corrected (i.e., calibrated) wavelength was compared with the measured (experimental) wavelength in five separate tests. The corresponding results are presented in Table 1. The interferometer system has a systematic error of 0.004491 nm. Correcting for this systematic error, the wavelength is found to have a mean normalized accuracy of $(\Delta\lambda/\lambda)$=1.05978E-09. The instantaneous corrected wavelength stability is less than 1.54E-06.

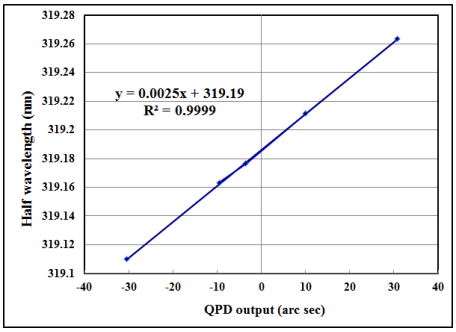

Fig. 10: Relationship between wavelength and QPD angle output.

Table 1: The correct wavelength (Calibrated) compared with measured wavelength (Experiment), unit: nm

Times	Calibrated (λ)	Experiment (λ')	Error	$(\Delta\lambda/\lambda)$%	Error-0.004491	$(\Delta\lambda/\lambda)$%
1	319.180911	319.176123	0.004788	1.50002E-05	0.000297	9.29581E-07
2	319.163887	319.159738	0.004149	1.30001E-05	-0.000342	-1.07125E-06
3	319.183570	319.179102	0.004469	1.40003E-05	-0.000022	-7.018E-08
4	319.192082	319.187102	0.00498	1.56015E-05	0.000489	1.53139E-06
5	319.123447	319.119385	0.004072	1.27589E-05	-0.000419	-1.31424E-06
Avg			0.004491	1.40722E-05		1.05978E-09

3.3 Dual-axis autocollimator calibration

The measurement precision of the dual-axis autocollimator was evaluated using an HP5529A angular interferometer as a reference (see Fig. 11(a)). The mirror was rotated step-by-step through a pitch angle range of ±30 arc-sec and then the readings of autocollimator and interferometer are taken simultaneously. Figure 11(b) plots the residual error of the autocollimator over the range of ± 30 arc-sec for five separate tests. Applying a least-squares fitting technique, the residual error is found to have a value of ± 0.3 arc-sec over the considered range.

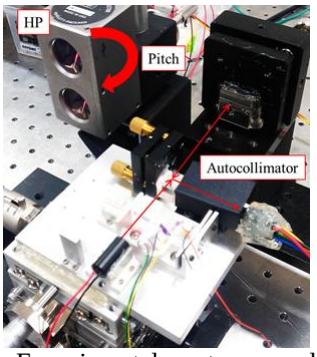

Fig. 11(a): Experimental setup used to calibrate autocollimator

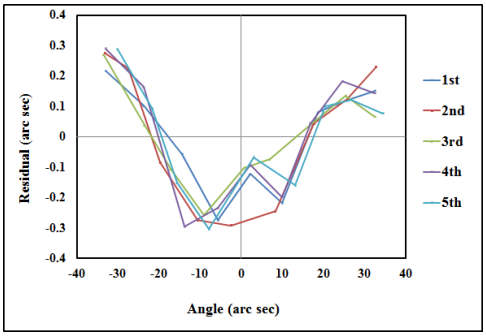

Fig. 11(b): Residual error of autocollimator

4. EXPERIMENTAL RESULTS

4.1 Abbe error compensation

Figure 12 shows the variation of the pitch deviation over a travel distance of 20 mm. The Abbe offset was determined to be 10.75 mm. This data served as reference and then was multiplied by the pitch deviation to obtain the Abbe error. Figure 13 shows the positioning results obtained with and without Abbe error compensation, respectively. It is seen that the positioning error is controlled to within ± 20 nm over a travel distance of 20 mm after compensation.

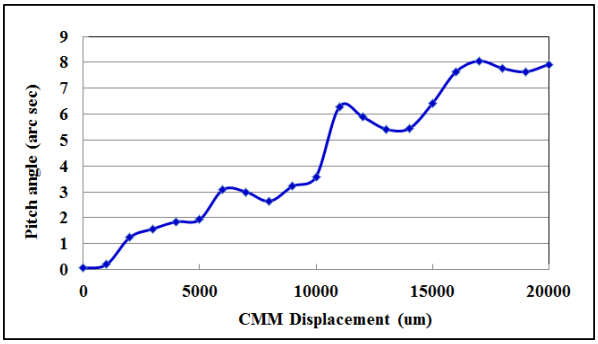

Fig. 12: Pitch deviation over 20 mm travel distance

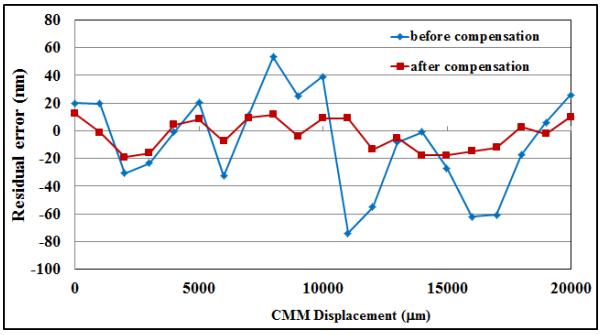

Fig. 13: Residual error with and without Abbé error compensation

5. CONCLUSIONS

This paper has presented the design of a high precision co-planar XY stage comprising two ultrasonic motors, associated drivers and two miniature multi-degree-of-freedom measurement system. Using the proposed MDFMS as the feedback sensor, the position reading can achieve nanometer level resolution. Besides, the Abbe error has been compensated from the measured pitch and yaw angles by the MDFMS. The experimental results have shown that the wavelength stability of the laser beam in the Michelson interferometer is less than 10^{-6}. In addition, it has been shown that the autocollimator has an accuracy of ± 0.3 arc-sec over the range of ± 30 arc-sec. Finally, the results have shown that the positioning error of the Co-planar XY stage is less than ± 20 nm over a travel distance of 20 mm.

REFERENCES

[1] H.T.H. Chen, W. Ng, and R.L. Engelstad, "Finite element analysis of a scanning x-ray microscope micropositioning stage", *Rev. Sci. Instrum.*, vol.63(1), pp. 591-594, 1992.

[2] R. Yang, M. Jouaneh, and R. Schweizer, "Design and characterization of a low-profile micropositioning stage", *Precision Engineering*, vol.18(1), pp. 20-29, 1996.

[3] P. Mckeown, "Nanotechnology-special article", *Proc. Nano-metrology in Precision Engineering*, pp. 5-55, Hong Kong, Nov. 1998.

[4] B.A. Awaddy, W.C. Shih, and D.M. Auslander, "Nanometer Positioning of a Linear Motion Stage Under Static Loads", *IEEE/ASME Trans. Mechatron.*, vol.3(2), pp. 113-119, 1998.

[5] H. Marth and B. Lula, "Development of a compact high-load PZT-ceramic long-travel linear actuator with picometer resolution for active optical alignment applications", *Proc. SPIE*, Vol. 5638, pp. 387-394, 2005.

[6] K.C. Fan, Y.T. Fei, et al, "Development of a low-cost micro-CMM for 3D micro/nano measurements", *Meas Sci Technol.*, vol.17(3), pp. 524-532, 2006.

[7] K. Takamasu, R. Furutani and S. Ozono, "Development of nano-CMM (Coordinate Measuring Machine with Nanometer Resolution)", *Proc XIV IMEKO World Congress.*, pp. 34-39, 1997.

[8] P. Yang and T. Takamura, et al, "Development of high-precision micro-coordinate measuring machine: Multi-probe measurement system for measuring yaw and straightness

motion error of XY linear stage", *Precision Engineering*, vol.35(3), pp. 424-430, 2011.

[9] K.S. Low and M.T. Keck, "Advanced precision linear stage for industrial automation applications", *IEEE Trans. Instrum. Meas.*, vol.52(3), pp. 785-789, 2003.

[10] S. Polit and J. Dong, "Development of a high-bandwidth XY nanopositioning stage for high-rate Micro-/Nanomanufacturing", *IEEE/ASME Trans. Mechatron*, vol.16(4), pp. 724-733, 2011.

[11] Y. Li and Q. Xu, "A Novel Piezoactuated XY Stage With Parallel, Decoupled, and Stacked Flexure Structure for Micro-/Nanopositioning", *IEEE Trans. Ind. Electron.*, vol.58(8), pp. 3601-3615, 2011.

[12] R. Koning, J. Flugge and H. Bosse, "A method for the in situ determination of Abbé errors and their correction", *Measurement Science & Technology*, vol.18(2), pp. 476-481, 2007.

[13] A.C. Okafor and Y.M. Ertekin, "Derivation of Machine Tool Error Models and Error Compensation Procedure for Three Axes Vertical Machining Center using Rigid Body Kinematics", *International J of Machine Tools & Manufacture*, vol.40(8), pp. 1199-1213, 2000.

[14] S.W. Kim, H.G. Rhee and J.Y. Chu, "Volumetric phase-measuring interferometer for three-dimensional coordinate metrology", *Precision Engineering*, vol.27(2), pp. 205-215, 2003.

[15] J.H. Jung, J.P. Choi and S.J. Lee, "Machining accuracy enhancement by compensating for volumetric errors of a machine tool and on-machine measurement", *Journal of Materials Processing Technology*, vol.174(1-3), pp. 55-66, 2006.

[16] H. Büchner and G. Jäger, "A novel plane mirror interferometer without using corner cube reflectors", *Meas. Sci. Technol.* vol.17(4), pp. 746-752, 2006.

[17] Q. Huang, X. Liu and L. Sun, "Homodyne laser interferometric displacement measuring system with nanometer accuracy", *In: 9th International Conference on Electronic Measurement and Instruments*, pp. 908-912. 2009

[18] S. Topcu, L. Chassagne, Y. Alayli and P. Juncar "Improving the accuracy of homodyne Michelson interferometers using polarization state measurement techniques", *Optics Communications*, vol.247(1-3), pp. 133-139, 2005.